ELSEVIER

Journal of Nuclear Materials 258–263 (1998) 1350–1355

journal of nuclear materials

Chemical segregation behavior of the low activation ferritic/martensitic steel F82H

R. Schäublin *, P. Spätig, M. Victoria

Technologie de la fusion Association Euratom-Confédération Suisse, Centre de Recherches en Physique des Plasmas, Ecole Polytechnique Fédérale de Lausanne, 5232 Villigen PSI, Switzerland

Abstract

The microstructure of the low activation F82H ferritic/martensitic steel has been investigated in the case of the heat treated and irradiated material. The irradiation has been achieved with 590 MeV protons in the PIREX facility to a dose of 0.5 dpa at a temperature of 523 K. The mechanical properties being intrinsically related to the chemistry of the metal, the understanding of the segregation behavior of the different alloying elements to microstructure defects, such as boundaries, is crucial. The segregation behavior to irradiation of both martensite laths and pre-austenite grain (PAG) boundaries is investigated using energy filtered transmission electron microscopy (EFTEM). It appears that Fe depletion of boundaries is observed in all cases, and the heat treated material experiences Cr segregation to boundaries, while the irradiated material experiences Cr depletion.

1. Introduction

Ferritic/martensitic steels have proved to be good alternatives to austenitic steels as candidates for the future fusion reactor structural components where doses above 100 dpa are expected. The chemical composition of the ferritic/martensitic steel F82H has been designed to obtain a reduced long term radioactivity. There are however a number of questions related to the changes in mechanical properties and to the swelling under irradiation that are still not fully answered. Recent studies on irradiation embrittlement of some ferritic steels have revealed that considerable shifts in the ductile–brittle transition temperature (DBTT) due to neutron irradiation appear together with an intergranular fracture mode [1]. This grain boundary embrittlement has been considered in [2] to be due to grain boundary precipitation of Mn and Si. Cr segregation to the pre-austenite grain (PAG) boundaries, and presumably to the martensitic lath boundaries as well, induced by the heat treatment prior to irradiation is believed to strengthen the boundaries [3]. It appears that irradiation depletes the grain boundaries of Cr, like in Fe–Ni–Cr stainless steels [3] and in commercial stainless steels [4], and it was shown in a ferritic steel Fe–Cr–P that Cr depletion of grain boundaries enhances the intergranular fracture mode [5].

A comparative study of the Fe and Cr segregation at grain boundaries is made here on the ferritic/martensitic F82H steel heat treated and specimens irradiated to 0.5 dpa with 590 MeV protons at a temperature of 523 K in the proton irradiation experiment (PIREX) facility located in the Paul Scherrer Institute of Villigen in Switzerland. The focus of this paper is on the chemistry of both martensite laths and grain boundaries. The mechanical properties and the microstructure investigation are presented elsewhere [6,7]. Although interface chemistry has been investigated with AES and using the subnanometric electron probe approach with EDS and (P)EELS in the past, the prospect of improving the spatial resolution, as well as preventing local changes in chemistry and low spatial statistics that are inherent to the probe approach, makes the use of energy filtered transmission electron microscopy (EFTEM) an attractive option. Moreover, the success of this technique in the study of Si segregation to grain boundaries in Cu [8] preceeds its use in the present work.

* Corresponding author. Tel.: +41 56 310 4082; fax: +41 56 310 45 29; e-mail: schaublin@psi.ch.

0022-3115/98/$19.00
PII: S0022-3115(98)00337-7

2. Experimental

The ferritic/martensitic F82H steel contains 7.65 wt% Cr, 2 wt% W, and Mo, Mn, V, Ta, Ti, Si and C below 1 wt% in sum total, and Fe for the balance [9]. The standard heat treatment (0.5 h at a temperature of 1313 K for the normalization, followed by 2 h at 1013 K for the tempering) has been applied in order to condition the material.

The TEM samples in the form of 100 μm thick 3 mm disks were prepared by electrochemical thinning with a solution of 10 vol% perchloric acid and 90 vol% methanol at a temperature of 0°C and a voltage of 30 V. TEM observations were conducted on a Philips LaB_6 CM20 operated at 200 kV, and the EFTEM observations were achieved on a Philips FEG CM300 operated at 300 kV and equipped with a (Gatan Imaging Filter) (GIF). Both microscopes belong to the Centre Interdépartemental de Microscopie Electronique of the EPFL of Lausanne in Switzerland. Part of the EFTEM observations were achieved on a JEOL 4000 FX equipped with a GIF and operated at 400 kV that is located in the Department of Materials Science and Metallurgy of the University of Cambridge.

The EFTEM used here applies the technique of the three windows method with a post column filter. It sorts with a slit, or window, the transmitted electrons by their energy after passing through a magnet that is located below the main screen. The chemical map is obtained by subtracting from the image obtained using the electrons corresponding to a characteristic inner-shell loss edge for the element of interest an extrapolated background image derived from two images taken before the edge. This is done pixel by pixel in the digitized data, and in principle, the resultant loss image will show enhanced contrast in the regions rich in the selected element. There are however some inherent drawbacks to the method when a resolution of the order of the nanometer is expected.

The primary problem is the presence of conventional diffraction contrast due to the defect at which potential segregation is being examined. The diffraction contrast changes with the change in the energy loss at which the image is taken [10]. Consequently, there is an artificial contrast added on the chemical map that arises from the variation in the diffraction contrast from one image to the other. In order to circumvent that problem Hofer and Warbichler [11] proposed to acquire the images under a rocking beam illumination, which will average the diffraction contract to such an extent that the variation in diffraction contrast between images taken at the three different energy losses will be negligible. Unfortunately, this technique could not be applied to the present magnetic steel. This is presumably because when the electron beam is tilted in the presence of the magnetic field of the sample it deviates from the trajectory adjusted for optimal image quality which results in a low quality image.

In order to reduce the diffraction contrast problem, it is proposed here to select an objective aperture large enough to contain the transmitted beam and the main diffracted beam. This reduces the diffraction contrast and hence the aforementioned artefact on the chemical map. It should be noted that a compromise has to be found between a large enough objective aperture size that may reduce diffraction contrast and a smaller size that allows us to reduce spherical aberration [10]. It should be noted that the alignment of the images has to be done as precisely as possible in order to avoid subtraction of regions that do not correspond to each other.

The elements which are expected in our case to segregate to boundaries are Cr, Mn and Si [2,3]. Table 1 shows the energies of the main edges that are present in the EELS spectrum of the heat treated F82H material. The Mn, with a L edge at 640 eV, cannot be mapped using the three window method because one of the pre-edge images overlap the Cr L edge. The lower edge energies (C K edge, Si K edge and Mo M edge) prevent them to be used for mapping without difficulties because of the plasmon losses in this energy range that add to the signal and disturb the background extrapolation. The higher edge energies (Si L edge, Mo L edge and W M edge) present difficulties because the electron count rate is low and the acquisition times being higher the risk of sample drift and hence image blur is increased. The most suitable elements for chemical mapping are the Fe and the Cr. Their mapping was achieved using an energy window of 30–50 eV, with the L edge situated, respectively, at 708 and 574 eV, and with an acquisition time for the image of about 30 s. The three windows were taken at 495, 545 eV for the two pre-edge images and 600 eV for the post-edge image for the Cr, and at 643, 683 eV for the two pre-edge images and 733 eV for the post-edge image for the Fe.

Table 1
Main EELS edges in [eV] in the ferritic/martensitic F82H steel. K, L and M energy lines are presented together with the energy window width (ΔE) used for the acquisition of the presented results

Element	K	L	M	ΔE
Si	99.0	1839.0		*
Cr		574.0		30–50
Fe		708.0		30–50
Mn		640.0		*
Mo		2520.0	227.0	*
W			1809.0	*

* No corresponding chemical map acquired.

3. Results and discussion

Fig. 1, presented more in detail elsewhere [7], shows on low magnification micrographs the general microstructure of the F82H as heat treated (Fig. 1(a)) and irradiated (Fig. 1(b)). Both specimens have a common microstructure characterized by PAG boundaries and martensite lath boundaries.

In the following the chemical mapping results obtained by EFTEM of Fe and Cr at boundaries are presented. Fig. 2 presents the heat treated specimen and Fig. 3 shows the 0.5 dpa irradiated specimen. In the unirradiated specimen segregation of Cr is visible at lath boundaries as shown in Fig. 2(c) whilst there is a depletion of Fe (Fig. 2(b)). The diffraction contrast visible on the zero loss image (Fig. 2(a)) due to stress induced thin foil distortion is successfully reduced on both chemical maps. This can be seen for instance for the large black region below the interface on its left (Fig. 2(a)) that cannot be distinguished anymore on the chemical maps (Fig. 2(b) and (c)). The technique suggested here on the choice of the objective aperture proves to be successful, although there is still some residual diffraction contrast differences that add to the chemical signal as is observed when comparing the upper right corner of the zero loss image and the Cr map. It has to be noted that this residual contrast might be due to the drift of the sample during the acquisition of the images needed for the three window method. This is illustrated in Fig. 2(b) (Fe map) that presents a darker upper region relatively to the lower region, showing that the substraction of the extrapolated image and the

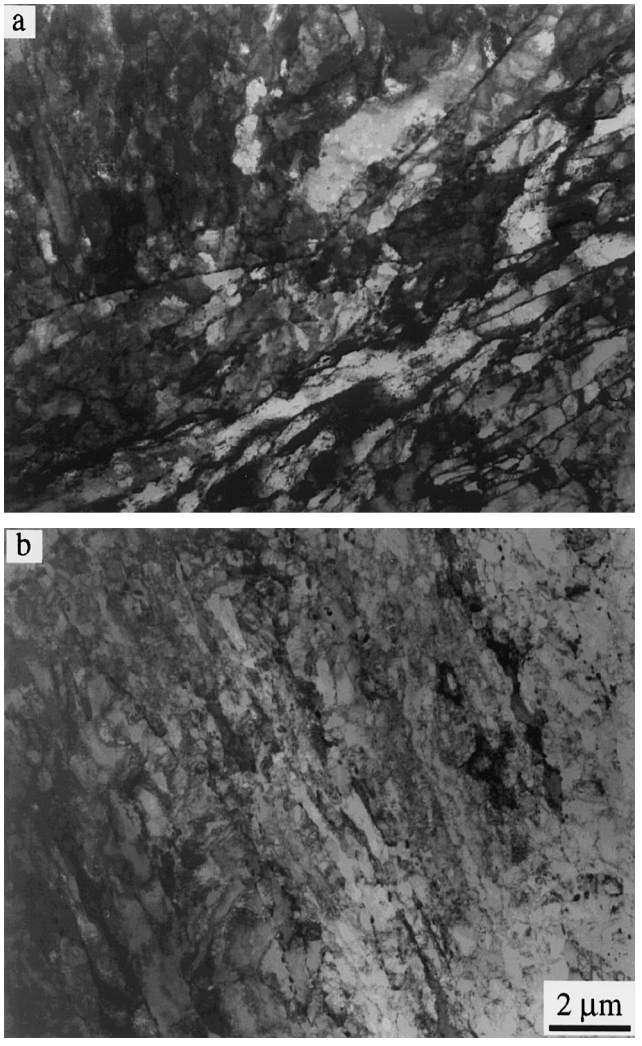

Fig. 1. TEM micrographs showing the basic microstructural features of the F82H material (a) heat treated, (b) irradiated at 0.5 dpa at 523 K.

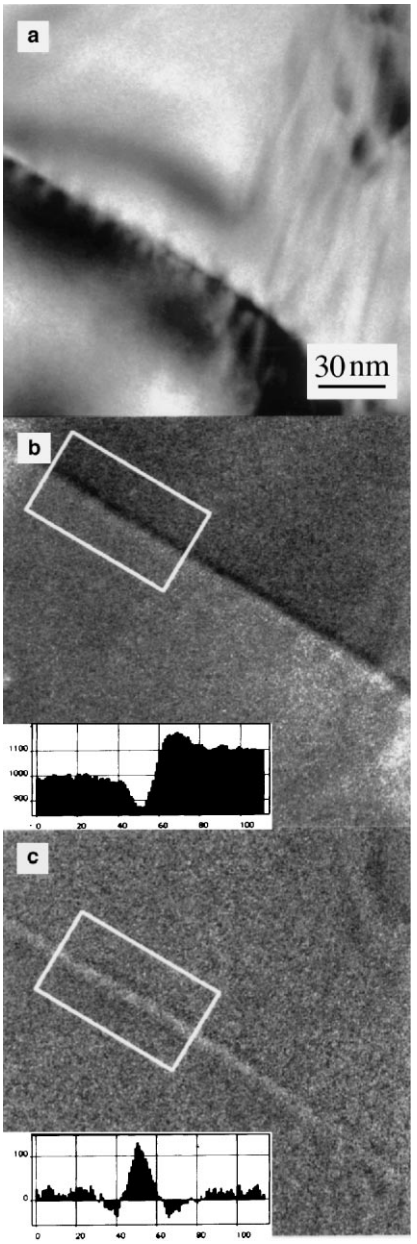

Fig. 2. Chemical mapping of the heat treated F82H material. (a) Zero loss image, (b) Fe map and (c) Cr map. The inserts show the image profile integrated in the respective boxes outlined in white. Horizontal axis is in pixels, vertical axis in counts.

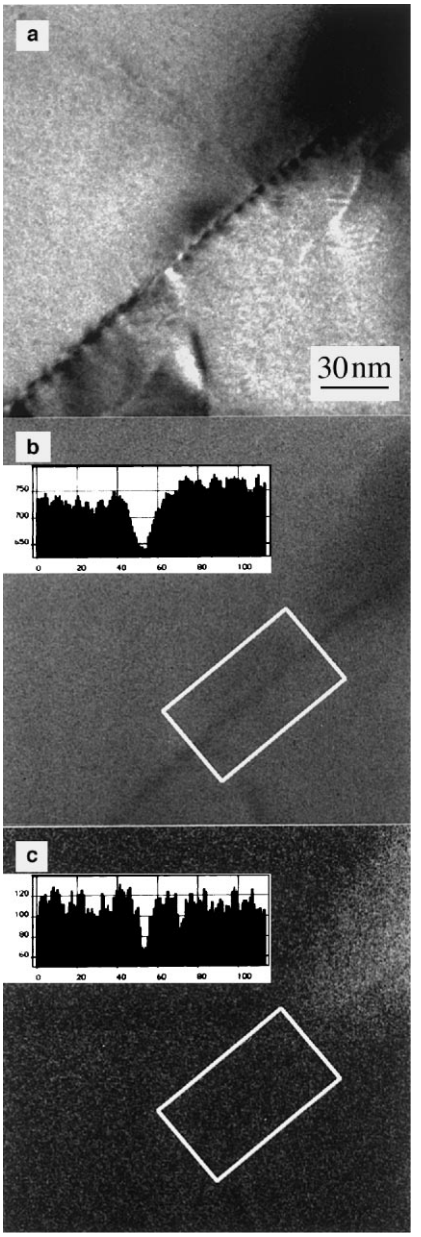

Fig. 3. Chemical mapping of the F82H material irradiated at 0.5 dpa at 523 K. (a) Zero loss image, (b) Fe map and (c) Cr map. The inserts show the image profile integrated in the respective boxes outlined in white. Horizontal axis is in pixels, vertical axis in counts.

post-edge image was not achieved on regions corresponding exactly, contrary to the case of Fig. 2(c) (Cr map) that presents no such drift trace. Moreover, the interface contrast of Fig. 2(b), showing depletion by a dark contrast, is underlined by a slightly lighter contrast that is not related to the chemistry but to drift. This slight drift effect has no influence on the conclusion because the integral of the count rates in the darker region is higher than in the lighter region of the interface, stressing the fact that there is depletion.

As mentioned earlier, there is a compromise to be found in the choice of the objective aperture with regard to diffraction contrast and resolution. Another issue that is of practical importance is that the diffraction contrast

is helpful to indicate the presence of thin interfaces. The fact that the interfaces present principally a diffraction contrast makes them difficult if not impossible to track them when the objective aperture is completely removed. But, again, even though diffraction contrast is helpful it has to be reduced to a minimum to avoid a perturbation of the chemical signal.

The irradiated specimen presented in Fig. 3 exhibits on a boundary a dark line in the Fe map (Fig. 3(b)). That indicates boundary Fe depletion. The Cr map (Fig. 3(c)) of the same boundary shows a dark line. Although the image contrast of Fig. 3(c) does not clearly display this dark line because of its noisiness, the image profile insert shows a significant intensity decrease at the boundary. This indicates boundary Cr depletion. The noisier image relatively to the heat treated case presented in Fig. 2(c) taken with the same experimental acquisition conditions suggests that the amount of depletion is lower than the amount of segregation observed prior to irradiation. This Cr depletion may explain that intergranular fracture mode is observed after irradiation [1]. Fig. 3 shows in the upper right corner of the three images a large and dark feature. Its dark contrast in the Fe map (Fig. 2(b)) and light contrast in the Cr map (Fig. 3(c)) suggest that it is a Cr carbide.

An in situ TEM tearing experiment has been conducted in order to observe the movement of a crack in relation with the microstructure features. By applying a rapid tilt to the sample holder the induced stress on the sample due to its immersion in the magnetic field of the objective lens allowed to bend the thin regions of the sample to such an extent that a crack could be initiated at the edge of the sample. The crack was then propagated progressively through the sample by further rapid tilts.

Fig. 4 shows the in situ TEM tearing experiment achieved on the as-received specimen. The crack visible in Fig. 4(a) runs close to the martensite lath boundary labelled 2. Interestingly, it seems that the crack is not visibly influenced by the presence of the carbides that are present on this martensite lath boundary. If the carbides are thought as being weakening points [12], the crack would then follow the martensite lath boundaries, leading to an intergranular fracture mechanism. It appears that this mechanism cannot be applied to fully explain the result of the present experiment. Effectively, even though the martensite lath boundary labelled 2 seems on Fig. 4(a) to be in the propagation direction of the crack, Fig. 4(b) shows that the crack did not follow the martensite lath boundary but turned downwards. In

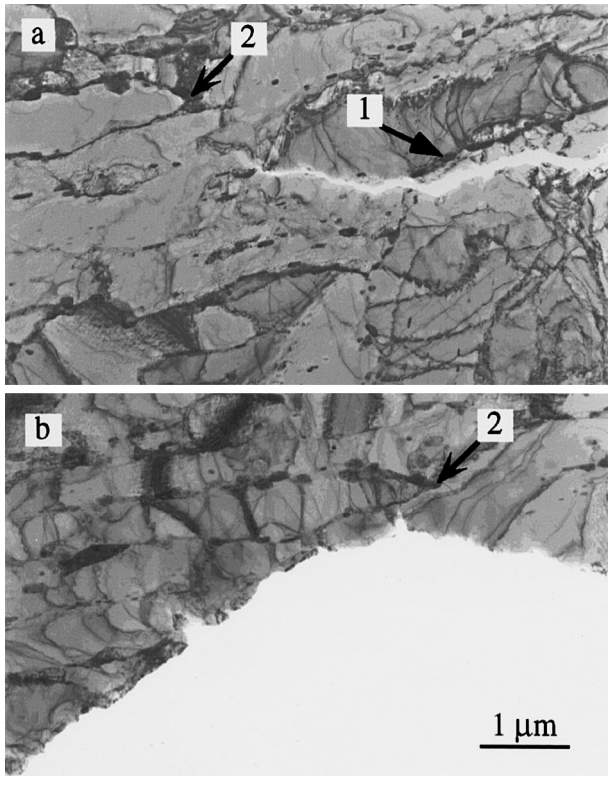

Fig. 4. In situ TEM tearing experiment on the heat treated F82H material showing starting crack on (a) and on (b) cutted specimen. Arrows show two boundaries decorated with carbides.

addition, the crack does not seem to follow any of the visible lath boundaries e.g. label 1. This TEM in situ experiment showing that the boundaries in the heat treated material are resistant to tearing might be explained by a boundary strengthening due to the observed Cr segregation. It shows for the least that they are not weakened by this segregation.

The fact that the irradiated material exhibits both Cr and Fe depletion shows that there is at least one element that was not determined in the present study that is segregated to the boundaries. Further work is being continued in this direction and on samples irradiated at higher doses.

4. Conclusion

1. Nanometric resolution in EFTEM is hindered in boundary chemistry investigation mainly by both diffraction contrast and image drift. It is suggested to choose an appropriate objective aperture that reduces diffraction contrast by including at least one of the major diffracted beams. EFTEM was applied successfully to the observation of boundary segregation.
2. EFTEM measurements show that the Cr segregates to both martensite laths and PAG's boundaries in the heat treated ferritic/martensitic F82H steel, while Fe is depleted from them. After irradiation at 0.5 dpa at 523 K Cr is depleted from the boundaries as well as Fe.

Acknowledgements

Prof. C. Humphreys is acknowledged for providing access to the JEOL 4000FX of the Department of Materials Science and Metallurgy of the University of Cambridge. Dr. C. Boothroyd is acknowledged for helpful interactions on the EFTEM application to this study.

References

[1] R.L. Klueh, D.J. Alexander, J. Nucl. Mater. 187 (1992) 187.
[2] A. Kimura, L.A. Charlot, D.S. Gelles, R.H. Jones, J. Nucl. Mater. 212–215 (1994) 725.
[3] S. Watanabe, N. Sakaguchi, K. Kurome, M. Nakamura, H. Takahashi, J. Nucl. Mater. 240 (1997) 251.
[4] S. Kasahara, K. Nakata, H. Takahashi, J. Nucl. Mater. 239 (1996) 194.
[5] C. Liu, K. Abiko, M. Tanino, Mater. Sci. Eng. A 176 (1994) 363.
[6] P. Spätig, R. Schäublin, S. Gyger, M. Victoria, these Proceedings.
[7] R. Schäublin, P. Spätig, M. Victoria, these Proceedings.
[8] R.E. Schäublin, W.M. Stobbs, Inst. Phys. Conf. Ser. 147 (3) (1995) 199.
[9] M. Tamura, H. Hayakawa, M. Tanimura, A. Hishinuma, T. Kondo, J. Nucl. Mater. 141–143 (1986) 1067.
[10] R.E. Schäublin, W.M. Stobbs, Inst. Phys. Conf. Ser. 147 (3) (1995) 203.
[11] F. Hofer, P. Warbichler, Ultramicroscopy 63 (1996) 21.
[12] C.L. Briant, Mater. Sci. Technol. 5 (1989) 138.